Digital nanoliter to milliliter flow rate sensor with in vivo demonstration for continuous sweat rate measurement

Journal:	*Lab on a Chip*
Manuscript ID	LC-ART-09-2018-000968.R1
Article Type:	Paper
Date Submitted by the Author:	18-Nov-2018
Complete List of Authors:	Francis, Jessica; University of Cincinnati College of Engineering and Applied Science, Novel Device Laboratory Stamper, Isaac; University of Cincinnati, Biomedical Engineering Heikenfeld, Jason; University of Cincinnati, Novel Devices Laboratory, Department of Electrical and Computer Engineering Gomez, Eliot; University of Cincinnati, Electrical Engineering and Computing Systems

Journal Name

ARTICLE

Digital nanoliter to milliliter flow rate sensor with *in vivo* demonstration for continuous sweat rate measurement

Jessica Francis[1], Isaac Stamper[1], Jason Heikenfeld[1,2], and Eliot F. Gomez[1]

Received 00th January 20xx,
Accepted 00th January 20xx

DOI: 10.1039/x0xx00000x

www.rsc.org/

Microfluidic flow rate sensors have constraints in both detection limits and dynamic range, and are not often easily integrated in lab-on-chip or wearable sensing systems. We constructed a flow rate sensor that easily couples to the outlet of a microfluidic channel, and measures flow rate by temporarily shorting periodic droplets generated between two electrodes. The device was tested with a dynamic range as low as 25 nL/min and as high as 900,000 nL/min (36,000x range). It was tested to continuously operate up to ~200 hours. The device is also simple to fabricate, requiring inexpensive parts, and is small enough to integrate into wearable devices. The required input pressure is as low as 370 Pascals. An ultra-low flow rate application was demonstrated for wearable sweat biosensing where sweat generation rates (nL/min/gland) were accurately measured in a human subject testing. The digital nanoliter device provides real-time flow rates for sweat rate and may have other applications for low flow rates in microfluidic devices.

Introduction

Sensors are at the heart of any interaction with the physical world, and their success or limitation propels or inhibits the advancement in many fields of science. This is particularly true in microfluidic and wearable technology which demand robust sensing technologies with low limits of detection and large dynamic ranges. One often over-looked sensing parameter is fluid flow rate. As lab-on-a-chip (LoC) and other microfluidic platforms scale down and shift into emerging applications, there will be an increasing need for integrated in-line flow sensors that detect nL to mL per min flow rates.

Sweat rate, for example, is an important parameter to measure in wearable sweat biosensing especially for the diagnosis and assessment of hyperhidrosis[1] and monitoring real-time fluid dehydration[2]. Sweat is also a rich source of analytes, (e.g. electrolytes, proteins, cortisol) that leak into the sweat duct from surrounding capillaries and interstitial fluid[3,4]. Continuous access to analyte monitoring leads to potential consumer products in wearable sensors for non-invasive diagnostics. However, sweat rate is a critical parameter for analyte monitoring since varying sweat rates directly affect analyte concentration.[5]

In our assessment of commercial and academic flow sensors[6–13], we found limitations in sensitivity or dynamic range as seen in Table 1. Most commercial sensors operate >3 µL/min with a 1 to 2-fold dynamic range. Furthermore, for sweat rate measurement, we have attempted to use commercially available sensors, but they suffer from additional noise when used for on-body sensing. One frequent method to measure flow rate is with a channel often containing multiple electrodes that short when fluid flows over it[7,8,14,15]. While the sensitivity can be low (<1 µL/min), such devices are limited by the length of the channel (i.e. unusable after the channel fills) or are not practical to integrate (i.e. long channel lengths and require patterned electrodes). The lowest flow rate sensors we found rely on optical cantilever[6] and capacitive sensing[7], but again the fabrication and integration procedures are more complex. There are other examples of wearable sensors such as a humidity sensor devices[16,17], sweat analyte sensors such as sodium[18,19], and an integrated channel sweat sensing patch[8]. The issue remains that humidity and analyte sensors do not directly measure fluid flow rate. One key device, demonstrated by Yang et al. uses similar digitizing principles to measure flow rate as the device now demonstrated in this work.[20] It is a textile-based device that collects sweat from the user's arm and wicks the fluid to short electrodes. The device is breathable and comfortable as a wearable. While perhaps one of the most practical sensor for sweat rate monitoring, the sensor could be improved upon to increase its dynamic range, limit evaporation, control movement, and expand its design to other LoC applications.

1 *Department of Biomedical Engineering, University of Cincinnati, Cincinnati, OH, 45221, USA.*
2 *Department of Electrical Engineering & Computer Science, University of Cincinnati, Cincinnati, OH, 45221, USA.*
† *Electronic Supplementary Information (ESI) available: [details of any supplementary information available should be included here]. See DOI: XX.XXXX*

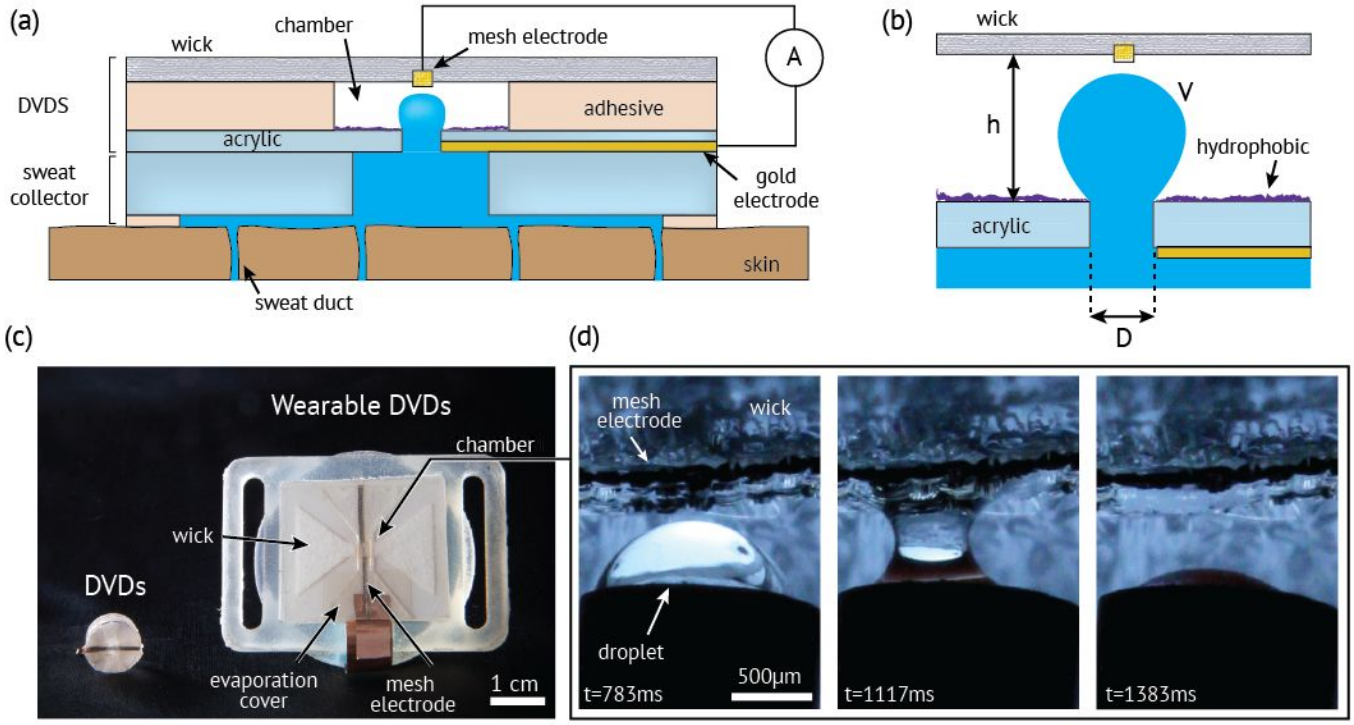

Figure 1 The DVDS flow sensor a) a side view of DVDS coupled to a wearable sweat collector; b) close-up of the chamber including critical parameters; c) photo of two different devices including a miniature version (left) and wearable version (right); d) demonstration of droplet breaking onto the mesh electrode.

In this work, we use digital droplets to measure fluid flow rate and demonstrate it for sweat rate monitoring, called the digital volume dispensing system (DVDS). DVDS operates by electrically detecting the frequency of droplet generation. As shown in Figure 1, fluid enters the device from the outlet of any pressure driven channel into DVDS where a droplet forms in a chamber. The droplet grows until it eventually shorts two electrodes before breaking onto a wick. Since the droplet volume is fixed by the chamber height (h), the droplet frequency directly measures the flow rate. The DVDS has a wide range of detection – tested as low as 25 nL/min and as high as 900,000 nL/min. This dynamic range is >100X larger than any commercial device listed in Table 1. The DVDS has a long lifetime that was tested continuously over 200 hours without missing a droplet generation event. Due to its small footprint, simplicity in fabrication, and rectifying volume (i.e. no backflow), the DVDS can be integrated or coupled to the outlet of any microfluidic device or fluid dispensing system, or a wearable device as demonstrated in this manuscript.

DVDS: Design and Theory

Table 1- Commercially available and academic flow rate sensors

Sensor	Low nL/min	High nL/min	Range	Type	ref
Intek Rheotherm Model 210	3.0e4	1.0e6	33X	Thermal	13
Sensiron SLG Liquid Flow Meter	1.5e3	2.0e4	13X	Mass Flow	12
Sensiron LPG10	1.0e6	1.5e6	1.5X	µfluidic	11
Omega FPR-1500	15e6	1.0e8	6.7X	Turbine	10
VVP Flow Sensor	3.0e5	3.6e6	12X	Differential Pressure	9
Optical Cantilever	6.1e3	1.3e6	213X	Optical Cantilever	6
Wearable Fabric	9.7e3	2.46e5	25X	Digital Droplet	20
Capacitive Channel Sensor	1	100	100X	µfluidic	7
DVDS (this work)	25	9e5	36000X	Digital Droplet	

The DVDS operates by (1) fluid entering a chamber through a small hole from the outlet of a pressure driven channel; (2) forming a capillary bridge that provides electrical conductivity between two electrodes; (3) a strong wicking event that breaks the capillary bridge that resets the process. The chamber and the inlet hole can be coated with a super hydrophobic surface, which causes the droplet to form a spherical cap or partial spherical shape in the chamber, as illustrated in Figure 1a and the close-up of the chamber in Figure 1b. Figure 1c shows a photo of two constructed and tested devices: a small stand-alone version that is only ~1 cm in diameter (left) and one that has been integrated into a wearable device (right). Figure 1d shows the droplet breaking onto the mesh electrode and Rayon wick. We demonstrated devices both with and without superhydrophobic coatings, and found superhydrophobic coatings to provide the most reliable in operation and therefore used for data collection in the paper. The video (See Supplemental files) and Supplemental Figure 1S

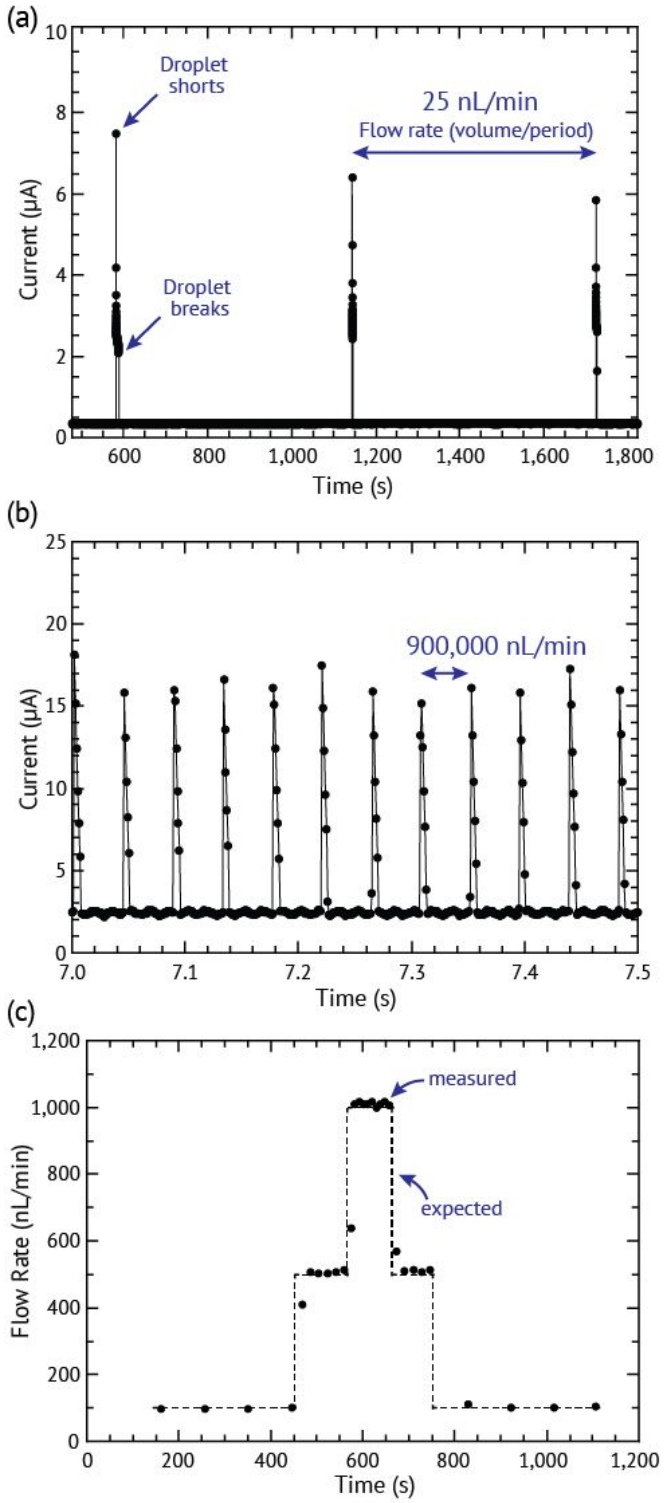

Figure 2 Demonstration of measured droplets a) 25 nL/min with current spike of a large period; b) 900,000 nL/min with current spike of a short period; c) demonstration of expected vs. measured flow rates.

shows a droplet that is nearly spherical when a super hydrophobic coating is used.

In Figure 1b, the chamber height (h) is made by layers of double-sided adhesive and PET film (see fabrication section for details). The chamber height controls the volume of the droplet (V). The volume could easily be reduced if photolithography or injection molding processes are employed. The diameter of the inlet (D) is a flexible parameter, but a smaller D encourages the droplet meniscus bridge to break near the inlet, and thus allowing h and V to remain small[21]. The only other constraint is D must be smaller than the outlet of the adjacent channel so that bottom electrode remains in constant electrical contact with the fluid.

Table 2 – Thickness variation and droplet volume

Thickness (μm)	Theoretical volume of a sphere (nL)	Actual Volume (nL)	Std Dev of Calibrated Device (nL)
447	46.8	128	4.88
664	153	193	5.18
951	450	491	8.82
1168	834.3	872.8	23.53

The electrode at the top of the wick only makes contact when the droplet reaches a particular volume. A small voltage (0.5 V) is applied to the electrodes and the current is measured over time. Droplets short the electrodes resulting in a brief current spike of several μA and 50-500 ms duration, as shown in Figure 2a and 2b. The flow rate is calculated given the known volume: flow rate = volume/T, where the period (T) is the time between the spikes. As the droplet emerges in the channel, an effective contact angle (θ) of the droplet with the substrate plane right before the droplet breaks onto a wick. A perfect sphere is never reached before a capillary bridge is formed, and the volume of each droplet can be calculated[22], *viz*.

$$Volume = \frac{4\pi}{3} r^3 (2 - 3\cos(\theta) + cos^3(\theta))/4 \qquad (1)$$

However, the theoretical volume calculated in Table 2 used the spherical equation (where r=h/2) which was in better agreement with the actual volume recorded. For small thicknesses, the theoretical volume deviated from the average volume (46.8 vs 128 nL, respectively). For thicknesses larger than 447μm, the theoretical volume closely matched the average experimental volume. We believe that the deviation from the spherical volume is due to meniscus break of the water droplet extending into the channel, (i.e. fluid pulled out of the DVDS outlet beneath the droplet) which could be corrected by reducing D.

The droplet in the DVDS is not easily dislodged due to its small volume (10 – 100's of nL) and high surface tension. The calculated Bond number is 0.057 for the largest well layer we tested (h=1168 μm). Therefore, in this system surface tension is a dominating factor over gravity. Because the subjects move a minimal amount, this is fine for *in vivo* testing, however, body movements can cause accelerations many times gravity (G) [23]. To account for this, and keep the Bond number less than 1, the greatest

h should be 2400 µm at 5G and 1600 µm to account for 10G acceleration.

The height of the chamber (see Figure 1b) can be adjusted to allow for different droplet volumes that will change the droplet frequency for larger or smaller flow rates. A positive Laplace pressure ($\Delta p = 2\gamma/r$) is required to create this droplet, and for an input diameter of D = 790 µm and for water ($\gamma = 73\ mN/m$), the maximum pressure required for operation is a spherical cap with a radius of 395 µm and a pressure of ~370 Pa. For any case of inflating the droplet beyond a spherical cap, the effective droplet radius only increases, and therefore the spherical cap represents the maximum required input pressure.

Fabrication

The DVDS fabrication starts with an acrylic sheet (1.5 mm thick) laser cut into a rectangle 25 x 29 mm with a 0.79 mm diameter hole in the center. The channel that couples to the DVDS must have a diameter larger than 0.79 mm so that the fluid contacts the bottom electrode (see Fig. 1a). The bottom electrode is a 50 nm gold film sputtered onto the bottom of the DVDS substrate. Afterwards, a super hydrophobic coating (Rust-Oleum NeverWet®) was spray applied to the top of the acrylic through a shadow mask to only coat the chamber area (3 mm diameter hole). NeverWet® was applied by spraying two coats of the base coat with 30 minutes between coats, and after 30 minutes spray three coats of the top coat with a few minute intervals according to the manufacturer instructions for the product. It was allowed to dry for at least 30 minutes before testing. The contact angle is between 160°-175° according to the manufacturer which classifies it as a superhydrophobic surface. It is important to note that the droplet never reaches this high of an angle before it breaks onto the wick, but the hydrophobicity helps maintain better droplet consistency. The chamber consists of laminated sheets of 5 mil (0.127 mm) PET, 3M 1522 adhesive (0.16 mm), and the 3M 9965 microfluidic tape (0.09 mm). In each layer, a hole 3 mm in diameter is laser cut in the thin laminated sheets (1522 adhesive, PET, 9965 microfluidic tape). The laminated sheets were adhered to the substrate e.g.: acrylic/1522/PET/9965. Different thicknesses (h) could be constructed by stacking additional film/tape on top or removing layers in different configurations to get the desired thickness. The only requirement being that the top of the chamber must have adhesive such that an electrode and a wicking layer of rayon could be placed on top of the stack. Afterwards a layer of PET is placed on top of that to prevent unwanted evaporation over the chamber.

We experimented with several different types of electrode materials for the top electrode including a wire

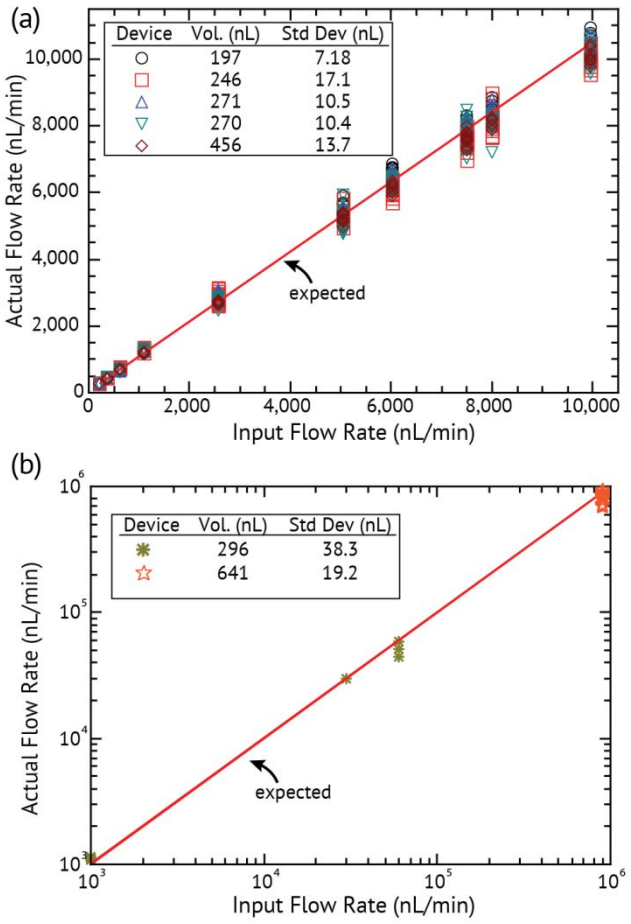

Figure 3 - *In vitro* validation of input flow rate to the measured flow rate of DVDS: (a) low flow rates 100 – 10,000 nL/min; (b) high flow rates 1,000 – 900,000 nL/min.

mesh (Ni plated nylon), a thin tungsten wire, and gold coated Rayon. We found that the droplet broke very quickly (<10 ms) using either the gold coated Rayon or thin tungsten wire. For our application, we elected to use the Ni mesh electrode which caused the droplets to break in 50-500 ms which was easy to detect at a lower sampling rate. The electrode (0.8 mm x 25 mm) was laser cut from woven conductive fabric (200 x 200 x 0.08 mm copper and nickel plated nylon; Adafruit) and was placed on top of the 9965 adhesive such that the electrode passed over the hole to make contact with the droplet. With the mesh electrode in particular, we noted the first droplet typically takes longer than normal (sometimes seconds) to break, but as soon as it wets, a water film forms within the mesh (which is visible in Figure 1d and more prominent on the Supplemental Videos) and subsequent droplets break as expected under 500 ms.

For the on-body device, the DVDS device was placed into a 3-d printed sweat collector (Formlabs Form II 3d printer and clear FLGPCL04 photopolymer resin). Data from tests was run through a Mathematica script to find

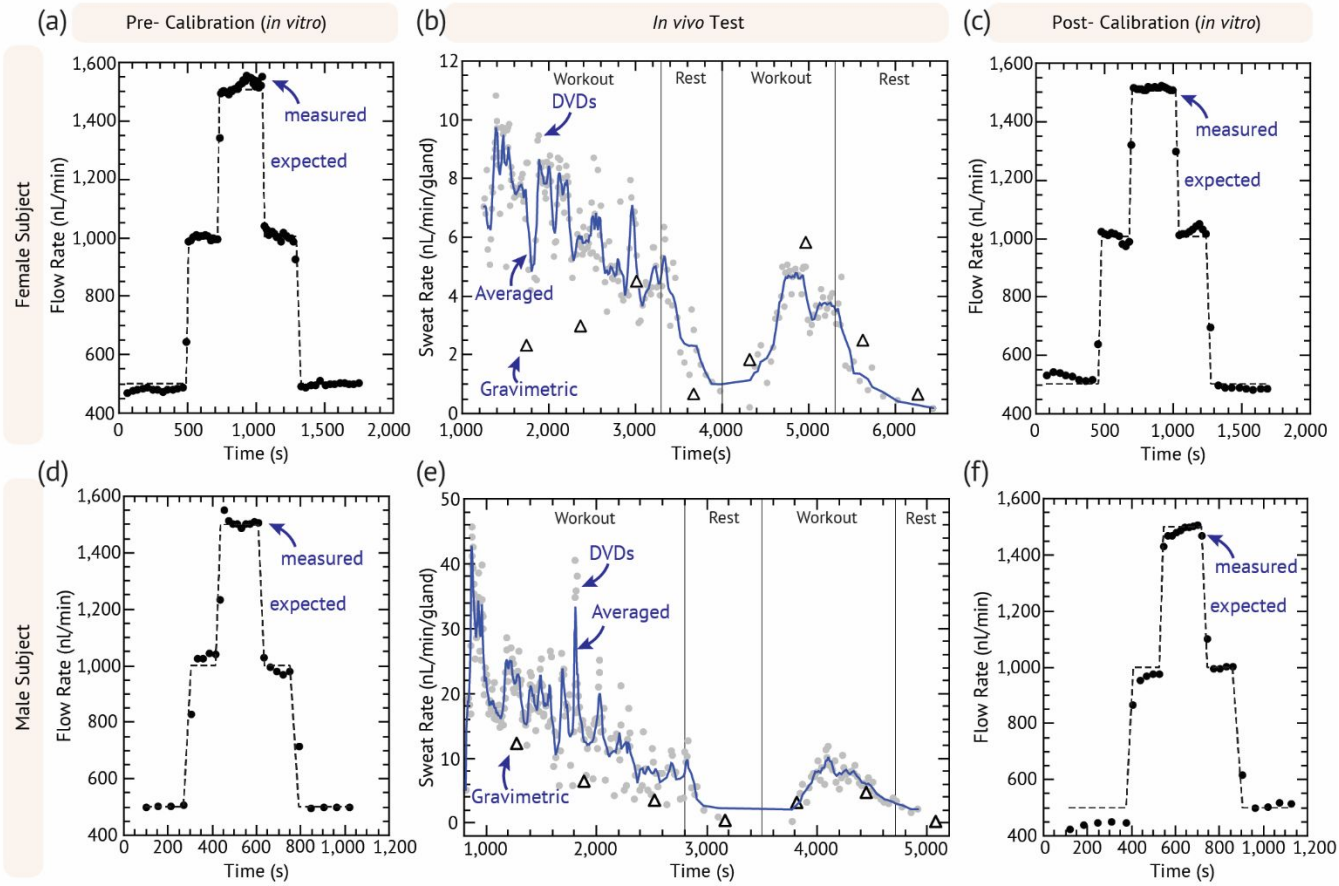

Figure 4 Exercise sweat test for a female subject (a-c) and male subject (d-f). Pre- calibrations (a and d) and post calibrations (c and f) to validate the device showing expected (dashed) and measured (solid dots) data. For on-body testing (b and e for female and male, respectively) shows DVDS (gray circles) and gravimetric data (white triangles). The moving average of the DVDS data is also shown (blue line).

the peaks and time of each droplet. The dimensions for this on-body device are provided in the on-line supplementary file.

In vitro Validation

The *in vitro* testing setup used a 1 mL Hamilton™ 1000 Series Gastight™ Syringes connected to a dispensing needle that attached directly to the hole of the sweat collector and to the DVDS. The syringe pump was a model 110 from KD Scientific. The sampling software was Gamry Reference 600 Potentiostat/Galvanostat/ZRA. The *in vivo* testing used laser cut 1522 adhesive on the bottom of the collector to the skin and a Velcro® arm band was used to fix the collector. The area of skin under the collector was 2.2698 cm^2. Details of the gravimetric holder can be found in Simmers *et al.*[24].

The syringe contained 50 mM of NaCl and was controlled using a syringe pump. A voltage (0.5 V) was applied and measured with chronoamperometry using the Gamry connection to the electrodes. The pump was set at various flow rates and examples of the output are shown in Figure 2 and Figure 3. Figure 2a plots the lowest successful flow rate at 25 nL/min with each droplet shorting every 10 minutes (device parameters: volume = 226 nL; h = 0.664 mm; D = 0.79 mm, see Figure 1b).

Lower rates were attempted, but these failed due to the wick drying out. We believe that even lower flow rates could easily be overcome by reducing h and

D and preventing evaporation using a larger evaporation cover. Photolithography or other more precise fabrication techniques could also reduce h but was out of the intended scope of this study. Figure 2b shows a device tested at 900,000 nL/min showing 12 discrete droplets detected in 0.5 second (Device parameters: volume = 632 nL; h = 1.168 mm;

D = 0.79 mm). At high rates the device works until the wick fails to remove liquid from the chamber, thus flooding the chamber. Faster rates could potentially be achieved by increasing h to reduce the droplet frequency and by using improved materials that support higher wicking pressures and flow rates.

Our lamination-based fabrication method resulted in slight variations in h that affect the volume of the droplet. Droplet volumes from device to device can vary as much as several hundred nL due to small changes in chamber height (h) introduced by manual fabrication. Therefore in this work, every device required calibration prior to use. In the calibration setup, a syringe pump runs through a series of flow rates (e.g. 100, 500, 1000, 500, and 100 nL/min) ensuring that at least 5 droplets are detected at

each flow rate. The period and flow rate are then used to determine the volume of the droplet. Figure 2c plots expected versus measured flow rates in a calibration. Different well layer thicknesses were built and tested and the results are summarized in Table 2. Once a device is calibrated and the volume of the droplet determined for that device, the volume is extremely reliable and repeatable (SD = 4.89 nL for h = 447 μm and SD = 23.53 nL for h = 1168 μm) over the lifetime of the device. It is certainly possible to imagine a calibration-free device where device tolerances are tightly controlled and thus the device is calibrated only at the factory.

In order to test the range and accuracy, devices were run at intervals from 100 to 900,000 nL/min. Figure 3 plots the input flow rate of a syringe pump versus the actual flow rate as measured by DVDS. In Fig. 3a, five separate devices were used in the experiments for flow rates 100 to 10,000 nL/min. Each flow rate has at least 5 data points collected. Every device is calibrated before the experiment to determine the volume of the droplet. The insets show the volume for each device (based on the calibration) and that volume is used to calculate the flow rate from the measured period. The standard deviation for each device is shown as the error of the droplet volume for the entire experiment set with a very low SD ≤ 17.1 nL. Small changes in the droplet volume can result in significant changes in the flow rate (e.g. at 8000 nL/min we expect a droplet every ~1845 ms, but droplet volume changes range ±200ms). But the droplet consistency allows excellent accuracy over the range.

Figure 3b shows two devices performing at higher flow rates from 1,000 to 900,000 nL/min. Even at high flow rates, the results show that the DVDS have higher accuracy that follow the expected rate throughout the entire range.

A device was run at steps of 1000, 30000, and 60000 nL/min. Each flow rate had at least 15 data points collected. The calibrated droplet size was 296 nL with a SD = 38.3 nL. A different device was run at 900,000 nL/min for 15 seconds; acquiring about 300 data points. The calibrated droplet size was 641 nL and the average volume over this test was 669 nL with a SD = 19.2 nL. The droplet volume remained remarkably consistent considering the extremely high flow rate, averaging 861,000 nL/min with a standard deviation of the flow rate equal to 24,900 nL/min.

To determine the effect of gravity on the volume of the droplet, calibration tests were performed with the syringe horizontaland then vertical for the thickest well layer (1168 μm) (see Supplemental Figure 3S). The average volumes calculated for the droplet were different by less than 10 nL. As a result, we concluded that orientation and gravity have little to no effect on the volume of the droplet. This can be expected because of the low Bond number of the droplet.

Finally, to test the longevity of the device the pump was run (device parameters: volume = 190 nL; h = 0.664 mm; D = 0.79 mm) continuously at 100 nL/min with daily calibration tests until the device failed. There was no longer an electrical signal detected. The device failed when salt crystalized onto the wick and into the chamber that eventually impeded droplet formation and breaking. When the device was taken apart, there was visible crystallization on the bottom and sides of the chamber and on the wick. The experiment ran for 200 hours (see Supplemental Table 1S). One could image a device constructed with a 1 mL wick and sealed to prevent evaporation that could potentially last for 10,000 hrs at 100 nL/min.

In vivo Validation

Human subjects testing was performed under the guidance of the University of Cincinnati's Human Research Protection Program (ID# 2016-4386 approved by the UC Institutional Review Board.) All human subjects provided informed consent. DVDS was coupled to the outlet of a 3D printed sweat collection device using 3M 1522 tape and calibrated using the standard (*in vitro)* calibration protocol. The device chamber height (h) was fabricated based on expected sweat rate of the subject: heavy sweating (device: volume =475 nL; h = 0.951 mm) or light sweating (device: volume =221 nL; h = 0.664 mm). The sweat collection device was strapped to the dominate forearm using elastic bands and 1522 tape. The collection area covers 2.2698 cm^2 of skin. Each DVDS was calibrated before and after experimentation as shown in Figure 4. As calculated previously, DVDS requires input pressures of 100's of Pa so a logical question is whether sweat generation can provide such pressure. Sweat generation is powered by osmotic pressures of 1's to 10's of kPa, easily satisfying this device requirement.[25]

During *in vivo* testing, gravimetric samples were also collected and measured, using pre-weighed 1.06 cm diameter laser cut TechniCloth™ nonwoven wipes (TX609, Texwipe, Kernersville, NC) disks. The disks were strapped to the subject's arm using an acrylic holder following similar previous protocols[24].

Subjects were asked to work-out on an exercise bike at a moderate rate. Each device had a dead volume of the DVDS and sweat collector is 2.9 and 25.6 mm^3, respectively, which in total took about 15 to 20 min to fill depending on how fast the subject began sweating. The gravimetric measurements began as soon as the DVDS detected the first droplet. Each gravimetric sample is collected for 10 min and then immediately weighed. The subject exercises at the same rate for 30 min and three gravimetric measurements are taken while the DVDS

measurements are continuously collected. The subject then takes a 10 minutes rest with one parallel gravimetric measurement. The subject is asked to begin exercising again for 20 minutes with two more gravimetric measurements during that time. The subject then stops exercising and a final gravimetric measurement is taken. The DVDS and sweat collection device is then calibrated a second time after it is removed from the subject by connecting it to a syringe pump as described above. The chronoamperometry data from this test is run through the script that finds each current peak and calculates the time differences between each peak. The calibration data is used to calculate the volumetric flow rate of the *in vivo* data, which are the plots shown in Figure 4.

Discussion

Figure 4(a-c) and 4(d-f) show the results of an exercise test of a female and male subject, respectively. The results of other tests are shown in Supplemental Figure 2S. Figure 4a and 4d show the pre-calibration data and Figure 4c and 4f show the post-work out calibration. Figure 4b and 4e plot the raw DVDS data; the moving average; and gravimetric results every 10 min. The *in vivo* experiments had more variation than the *in vitro* syringe pump experiments, but the pre- and post-calibration data confirmed that the device was working as expected. Subjects had normal arm movement during the workout and they were occasionally asked to flex their muscles or move their arm to see if there were any motion effects or if the droplet could be dislodged, and none were directly observed. Occasionally during a gravimetric change, we would observe changes in rate, but this was not always consistent. This could be due to pressure changes affecting the wearable device.

The sweat rate was calculated by gland density, considering that the average gland density 100 glands/cm^2 for the forearm (i.e. ~226 glands) [26]. In Figure 4b, the female subject started with a sweat rate of ~10 nL/min/gland which decreased steadily to ~5 nL/min/gland in the first workout period. The sweat response was delayed such that the lowest rate for the female subject was achieved nearly 1000 s after the rest period. The rate peaked at 5 nL/min/gland almost 800 s after the start of the second workout.

In Figure 4e, the male subject had a high rate at about 45 nL/min/gland, which then steeply dropped after several minutes to ~20 nL/min/gland. The sweat rate quickly dropped zero in 200 s after the start of the rest period, which was must faster than the female subject. After the rest, the flow rate peaked at 10 nL/min/gland about 600 s into the second workout. The initial measured rate for the male subject is unexpectedly high[25].

We speculate that air bubble formation in the sweat collector device could be causing the unexpected results during the initial phases of *in vivo* device use. When the device is first placed onto skin, undoubtedly air gaps and pockets exist, which can be pushed forward as sweat is generated. Such air bubbles could cause false high-readings of sweat generation rate (e.g. partial droplets) and could cause erratic changes in measured sweat generation rate as they pass through the system. We therefore believe the later data with reduced noise in the second workout represent most accurately normal operation of the device, especially since pre- and post-calibration data are well matched. In addition, since the DVDS has rectifying ability there cannot be backwards flow into the device resulting from arm movement. However, some of the variation in flow rate may be due to body movement or other physiological factors that we have not yet considered here.

Certain design considerations of DVDS can improve performance depending on the intended application. Lower flow rates could be achieved if the chamber is designed for smaller droplet volumes. One major challenge for smaller flow rates was the wick drying out, which causes a longer breaking time and changes the volume of the droplet. In this case, it may make more sense to use a more hydrophilic electrode or to gold coat the Rayon to decrease the droplet break time. Also, as mentioned previously, more sophisticated methods for device construction would have impact factory-calibration and potentially improving the range of flow rates that could be detected.

Lifetime of the device depends entirely on management of the fluid. Since this particular design intended to evaporate the water so as not to over saturate and potentially flood the chamber, the major problem was the salt build-up in the wick, eventually building up into the chamber. Effective management of fluid requires a balance of keeping the active site wet (in the case of the mesh electrode), and directing enough fluid away so that salt does not precipitate and clog the chamber. Such design considerations require a foreknowledge of flow rate range, droplet volume, and evaporation rate, however simple efforts to prevent evaporation or increasing the reservoir wick volume may improve the lifetime from weeks to months.

Conflicts of interest

Jason Heikenfeld has an equity interest in Eccrine Systems, Inc., a company that may potentially benefit from the research results, and also serves on the company's Board. The terms of this arrangement have been reviewed and approved by the University of Cincinnati in accordance with its conflict of interest policies.

Acknowledgements

Funding was made possible by the Ohio Federal Research Network through the Ohio Department of Higher Education (ODHE) and Wright State Applied Research Corporation (#WSARC-1077-700) and the Air Force Research Labs Award #FA8650-15-C-6625, and from NSF EPDT Award #1608275.

The authors would also like to thank Eccrine Systems Inc. particularly Mikel Larson and Dr. Michelle Hoffman for recommending flow tests in Figure 3 and good conversations on device fabrication optimized for sweat rate monitoring.

Notes and references

1. Atkins, J. L. & Butler, P. E. M. Hyperhidrosis: A Review of Current Management. *Plast. Reconstr. Surg.* **110,** 222–228 (2002).
2. Brake, D. J. & Bates, G. P. Fluid losses and hydration status of industrial workers under thermal stress working extended shifts. *Occup Env. Med* **60,** 90–96 (2003).
3. Jia, M., Chew, W. M., Feinstein, Y., Skeath, P. & Sternberg, E. M. Quantification of cortisol in human eccrine sweat by liquid chromatography - tandem mass spectrometry. *Analyst* **141,** 2053–60 (2016).
4. Jajack, A., Brothers, M., Kasting, G. & Heikenfeld, J. Enhancing glucose flux into sweat by increasing paracellular permeability of the sweat gland. *PLoS One* **13,** e0200009 (2018).
5. Heikenfeld, J. *et al.* Wearable sensors: modalities, challenges, and prospects. *Lab Chip* **18,** 217–248 (2018).
6. Lien, V. & Vollmer, F. Microfluidic flow rate detection based on integrated optical fiber cantilever. *Lab Chip* **7,** 1352 (2007).
7. Temiz, Y. & Delamarche, E. Sub-nanoliter, real-time flow monitoring in microfluidic chips using a portable device and smartphone. *Sci. Rep.* **8,** (2018).
8. Nyein, H. Y. Y. *et al.* A Wearable Microfluidic Sensing Patch for Dynamic Sweat Secretion Analysis. *ACS Sensors* **3,** 944–952 (2018).
9. VVP Technology – Dynamic Devices. Available at: http://dynamicdevices.com/vvp-technology/. (Accessed: 10th August 2018)
10. PTFE Liquid Flow Sensors. Available at: https://www.omega.com/pptst/FPR1500.html#description. (Accessed: 10th August 2018)
11. LPG10 - Liquid Flow Sensor | Sensirion. Available at: https://www.sensirion.com/en/flow-sensors/liquid-flow-meters/page/lpg10-planar-miniature-flow-sensors/. (Accessed: 10th August 2018)
12. SLG - Liquid Flow Meter | Sensirion. Available at: https://www.sensirion.com/en/flow-sensors/liquid-flow-meters/slx-standalone-liquid-flow-meters/uhplc-liquid-flow-sensors-for-ultra-low-flow-rates/. (Accessed: 10th August 2018)
13. Liquid Flow Meters - Rheotherm. Available at: https://intekflow.com/flow-measurement-instruments/low-flow-meters-liquid/. (Accessed: 10th August 2018)
14. Koh, A. *et al.* A soft, wearable microfluidic device for the capture, storage, and colorimetric sensing of sweat. *Sci. Transl. Med.* **8,** 366ra165 (2016).
15. Rogers, J. A. *et al.* A fluorometric skin-interfaced microfluidic device and smartphone imaging module for in situ quantitative analysis of sweat chemistry. *Lab Chip* **18,** 2178 (2018).
16. Sim, J. K., Yoon, S. & Cho, Y.-H. Wearable Sweat Rate Sensors for Human Thermal Comfort Monitoring. *Sci. Rep.* **8,** 1181 (2018).
17. Salvo, P. *et al.* A Wearable Sensor for Measuring Sweat Rate. *IEEE Sens. J.* **10,** 1557–1558 (2010).
18. Glennon, T. *et al.* 'SWEATCH': A Wearable Platform for Harvesting and Analysing Sweat Sodium Content. *Electroanalysis* **28,** 1283–1289 (2016).
19. Koh, A. *et al.* A soft, wearable microfluidic device for the capture, storage, and colorimetric sensing of sweat. *Sci. Transl. Med.* **8,** 366ra165 (2016).
20. Yang, Y. *et al.* Wearable microfluidics: fabric-based digital droplet flowmetry for perspiration analysis. *Lab Chip* **17,** 926–935 (2017).
21. Barkley, S., Scarfe, S. J., Weeks, E. R. & Dalnoki-Veress, K. Predicting the size of droplets produced through Laplace pressure induced snap-off. *Soft Matter* **12,** 7398–7404 (2016).
22. Wu, D. *et al.* Determination of contact angle of droplet on convex and concave spherical surfaces. *Chem. Phys.* **457,** 63–69 (2015).
23. Kimm, D. & Thiel, D. V. Hand Speed Measurements in Boxing. *Procedia Eng.* **112,** 502–506 (2015).
24. Simmers, P., Li, S. K., Kasting, G. & Heikenfeld, J. Prolonged and localized sweat stimulation by iontophoretic delivery of the slowly-metabolized cholinergic agent carbachol. *J. Dermatol. Sci.* **89,** 40–51 (2018).
25. Sonner, Z. *et al.* The microfluidics of the eccrine sweat gland, including biomarker partitioning, transport, and biosensing implications. *Biomicrofluidics* **9,** 031301 (2015).
26. Sato, K., Kang, W. H., Saga, K. & Sato, K. T. Biology of sweat glands and their disorders. I. Normal sweat gland function. *J. Am. Acad. Dermatol.* (1989). doi:10.1016/S0190-9622(89)70063-3

